Intramolecular Rearrangement Reactions of Tris-Chelate Complexes. I. General Theory and the Kinetics and Probable Mechanism of the Isomerization and Racemization of Tris(5-methylhexane-2,4-dionato)cobalt(III)

J. G. Gordon, II,[1] and R. H. Holm

Contribution from the Department of Chemistry, Massachusetts Institute of Technology, Cambridge, Massachusetts 02139.
Received February 9, 1970

Abstract: *cis* and *trans* isomers of the title compound, $Co(mhd)_3$ (**1**), have been completely separated by column chromatography and each has been partially resolved by chromatography on D-lactose. Rate constants for the isomerization reaction *cis* $\rightleftharpoons$ *trans* (having rate constants k_{CT} for the forward and k_{TC} for the reverse reaction) and the racemization of each isomer in chlorobenzene solution over the range 80–110° have been determined by a pmr method and polarimetry, respectively. All reactions are first order and the following rate constants (sec^{-1}) and activation energies (kcal/mol) have been obtained at 90°: $k_{CT} = 5.75 \pm 1.70 \times 10^{-5}$, 32.9 ± 1.4; $k_{TC} = 2.75 \pm 0.80 \times 10^{-5}$, 32.6 ± 1.6; $k_{rC} = 1.00 \pm 0.07 \times 10^{-4}$, 30.5 ± 0.6; $k_{rT} = 1.50 \pm 0.10 \times 10^{-4}$, 32.6 ± 0.8. The near identity of the activation energies is interpreted in terms of a common reaction pathway for isomerization and racemization. Isomerization reactions have been found to occur predominantly with inversion of configuration. A general treatment of the kinetics of these rearrangement reactions has been formulated in terms of six microscopic rate constants, values of which have been determined or estimated from experimental data. Reaction pathways involving no bond rupture (twist mechanism) and bond rupture (idealized trigonal-bipyramidal (TBP) and square-pyramidal (SP) transition states with the dangling ligand in equatorial or axial positions) have been analyzed. For each, topological correlation diagrams specifying all possible interconversions have been derived and ratios of isomerization and racemization rate constants predicted. Comparison of experimental and predicted ratios, together with the observations of simultaneous isomerization and racemization and stereoselectivity of the former process, has led to the exclusion of a twist mechanism and bond-rupture processes involving *only* TBP-axial, TBP-equatorial, and SP-axial transition states. The mechanisms consistent with the observed kinetics are of the bond-rupture type leading to formation of TBP-axial transition states together with smaller amounts of TBP-equatorial (~10%) or SP-axial (~20%). The CD spectra of partially resolved *cis*- and *trans*-$Co(mhd)_3$ are reported and compared with those of related complexes.

Tris-chelate complexes derived from unsymmetrical bidentate ligands can exist in two geometrically isomeric forms, *cis* (facial) and *trans* (meridianal), each of which is enantiomeric. These compounds constitute a widespread and important class of metal complexes and possess two properties of particular interest with respect to the present investigation and others currently in progress in this laboratory. One of these is the equilibrium distribution of isomers and the electronic and steric factors which affect it. Because the *cis* isomer has threefold rotational symmetry and the *trans* isomer no symmetry at all, the two isomers may be detected in the presence of each other and their relative proportions determined by nmr provided chemical shift differences are large enough. This is often the case and the available information reveals that complexes which are not sterically constrained from doing so usually, but not always, form a statistical (one *cis*/three *trans*) or nearly statistical distribution of isomers in solution. This situation obtains for the tris(β-diketonates) of cobalt(III)[2,3] and other trivalent metal ions.[2-5] On the other hand, tris complexes of vanadium(III) and cobalt(III) formed from ligands such as N-substituted salicylaldimines[6,7] and β-ketoamines[8] exist only in the *trans* configuration owing to steric destabilization of the *cis* isomer. Exceptions to this pattern are tris(monothio-β-diketonato)cobalt(III) and -vanadium(III)[5,9] and tris(salicylaldehydato)vanadium(III) complexes[7] which exist exclusively as the *cis* and *trans* isomers, respectively.

The other property of interest is that of intramolecular rearrangements, *viz.*, geometrical isomerization and racemization reactions.[10] The possible intermediates or transition states which might be implicated in these reactions have been considered in some detail recently.[11-15] Two types of reaction pathways may be distinguished. One involves no actual metal–ligand bond rupture and includes several processes which in the past have been referred to as the Bailar[16] or trigonal[11] twist and the Rây–Dutt[17] or rhombic[11] twist.

(1) National Science Foundation Predoctoral Fellow, 1967–1970.
(2) R. C. Fay and T. S. Piper, *J. Amer. Chem. Soc.*, **84**, 2303 (1962).
(3) R. C. Fay and T. S. Piper, *ibid.*, **85**, 500 (1963).
(4) F. Röhrscheid, R. E. Ernst, and R. H. Holm, *Inorg. Chem.*, **6**, 1315 (1967).
(5) J. G. Gordon, II, M. J. O'Connor, and R. H. Holm, in preparation.
(6) A. Chakravorty and R. H. Holm, *Inorg. Chem.*, **3**, 1521 (1964); A. Chakravorty and K. C. Kalia, *ibid.*, **6**, 690 (1967); A. Chakravorty and B. Behera, *ibid.*, **6**, 1812 (1967).
(7) F. Röhrscheid, R. E. Ernst, and R. H. Holm, *J. Amer. Chem. Soc.*, **89**, 6472 (1967).
(8) F. Röhrscheid, R. E. Ernst, and R. H. Holm, *Inorg. Chem.*, **6**, 1607 (1967).
(9) R. H. Holm, D. H. Gerlach, J. G. Gordon, II, and M. G. McNamee, *J. Amer. Chem. Soc.*, **90**, 4184 (1968).
(10) F. Basolo and R. G. Pearson, "Mechanisms of Inorganic Reactions," 2nd ed, Wiley, New York, N. Y., 1967, pp 300–334.
(11) R. C. Fay and T. S. Piper, *Inorg. Chem.*, **3**, 348 (1964).
(12) C. S. Springer, Jr., and R. E. Sievers, *ibid.*, **6**, 852 (1967).
(13) J. J. Fortman and R. E. Sievers, *ibid.*, **6**, 2022 (1967).
(14) E. L. Muetterties, *J. Amer. Chem. Soc.*, **90**, 5097 (1968).
(15) J. E. Brady, *Inorg. Chem.*, **8**, 1208 (1969).
(16) J. C. Bailar, Jr., *J. Inorg. Nucl. Chem.*, **8**, 165 (1958).
(17) P. Rây and N. K. Dutt, *J. Indian Chem. Soc.*, **20**, 81 (1943).

These twist mechanisms have been analyzed by Springer and Sievers,[12] who have provided the useful demonstration that these and other relative displacements of chelate rings not involving bond rupture may be envisaged as proceeding by means of twist motions of the three rings with respect to real or artificial threefold symmetry axes of the *cis* and *trans* isomers. The second type of reaction pathway involves bond rupture and the intermediacy of a five-coordinate structure, ideally a trigonal-bipyramidal[11,13,14] (TBP) or square-pyramidal (SP) entity with dangling axial or equatorial (basal) ligands.

One approach to an elucidation of the mechanism of intramolecular rearrangements of tris chelates is measurement of the kinetics of racemization and isomerization of *cis* and *trans* isomers of the same complex. This approach, which has also been recognized by others,[11,13] is applicable if the two processes proceed by the same mechanism and is easily appreciated by existing mechanistic considerations.[11-15] For example, a trigonal twist about the true threefold axis of the *cis* isomer will produce racemization without isomerization, whereas a twist about the artificial threefold axes (pseudo and imaginary[12]) will always effect racemization but not necessarily isomerization. Further, a TBP transition state will lead to simultaneous racemization and isomerization if the dangling ligand is axial but only isomerization if this ligand is in an equatorial position. The more detailed analysis which follows reveals that determination of the ratios of rates of isomerization and racemization for the *cis* and *trans* isomers has the potential of distinguishing among various reaction pathways, and, possibly, of leading to a unique choice of mechanism. In applying this approach two limiting types of systems are recognized. The first type is designated "slow," meaning that isomerization and racemization are sufficiently slow under ambient conditions that geometrical and optical isomers can be separated and the two processes studied at elevated temperatures by nmr and polarimetry, respectively. Slow systems are obviously those involving complexes of metal ions such as Co(III), Rh(III), Ir(III), Ru(II,III), Os(II,III), and, possibly, low-spin Fe(III). The second type of system is "fast," indicating that the two types of processes are too rapid to permit isomer separation and/or measurement of the rate of approach to equilibrium by these techniques. Fast systems are comprised of complexes of Al(III), Ga(III), In(III), V(III), and high-spin Mn(III) and Fe(III), among other metal ions.

The above approach to the investigation of intramolecular rearrangements of tris chelates has never been applied. Indeed, there is not one reported case in which rates of isomerization and racemization have been quantitatively determined for the same such complex. However, a limited amount of mechanistic information is available,[10] of which the most relevant to this study is that for tris(β-diketonato)metal(III) complexes.[18] The results of Fay and Piper[11] indicate that geometrical isomerization of $Al(tfac)_3$, $Ga(tfac)_3$, and $Cr(bzac)_3$ does not proceed by a trigonal twist mechanism, and that for $Al(tfac)_3$ bond rupture is likely to be involved in the process. In addition, the recent observation that linkage isomerization and racemization of $Co(triac)_3$ and $Co(triac)(acac)_2$ occur simultaneously but at different rates[19] may indicate that the latter process occurs at least in part by bond rupture, which is necessary for isomerization. Assessment of the significance of these results must await proof that both reactions are intramolecular, especially in view of the conclusion by Collman and Sun[20] that linkage isomerization reactions of closely related Co(III) β-diketonates are probably intermolecular.

The purpose of the present investigation has been to determine the rates and activation parameters for isomerization and racemization of *cis* and *trans* isomers of a suitable tris chelate of the "slow" type. Because of the body of kinetic-mechanistic information available[11,13,19] at the outset of this study, the general ease of separation of geometrical isomers of nonlabile species,[2,3,21] and the reported partial resolution of such species,[11,22,23] a tris(β-diketonate) complex, $Co(mhd)_3$ (**1**), was employed. The *cis* and *trans* isomers of

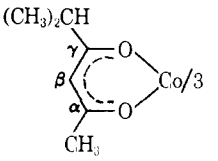

1

this complex have been separated and partially resolved and the kinetics and activation parameters for intramolecular isomerization and racemization measured in chlorobenzene solution. A complete account of the likely twist and bond rupture mechanisms is presented together with a general treatment of the kinetics of the two processes. Theoretical ratios of rate constants for these processes have been derived and shown to be dependent upon mechanism. These have been utilized to deduce the most probable mechanism(s) of the intramolecular rearrangements of **1**. Our investigations of "fast" systems[5,24] will be described in subsequent reports.

Experimental Section

Preparation of Tris(5-methylhexane-2,4-dionato)cobalt(III). A modification of the method of Hauser, *et al.*,[25] was used for the preparation of 5-methylhexane-2,4-dione. A 50% suspension of sodium hydride in oil (31 g, ~0.6 mol), washed twice with dry ether, was mixed with 110 ml (0.8 mol) of ethylisobutyrate and the resulting suspension warmed to 60°. Acetone (45 ml, 0.6 mol) diluted with 50 ml of dry 1,2-dimethoxyethane was added dropwise over 1 hr while maintaining the temperature at 55–65°. The dark red solution was heated at 75° for 50 min and then cooled to ~5°. Ethanol (20 ml) was added followed by 400 ml of water. The solution was extracted with ether (two 150-ml portions), acidified with 55 ml of cold concentrated hydrochloric acid, and extracted again with ether (four 100-ml portions). The combined ether extracts were washed with aqueous sodium bicarbonate and

(18) The following abbreviations of β-diketonate anions are employed throughout: acac, acetylacetonate; bzac, benzoylacetonate; tfac, trifluoroacetylacetonate; mhd, 5-methylhexane-2,4-dionate; triac, triacetylmethanide.

(19) U. Klabunde and R. C. Fay, Abstracts of Papers, 156th National Meeting of the American Chemical Society, Atlantic City, N. J., Sept 1968, No. INOR-37.

(20) J. P. Collman and J.-Y. Sun, *Inorg. Chem.*, **4**, 1273 (1965).

(21) R. J. York, W. D. Bonds, Jr., B. P. Cotsoradis, and R. D. Archer, *ibid.*, **8**, 789 (1969).

(22) T. Moeller and E. Gulyas, *J. Inorg. Nucl. Chem.*, **5**, 245 (1958).

(23) (a) J. P. Collman, R. P. Blair, R. L. Marshall, and L. Slade, *Inorg. Chem.*, **2**, 576 (1963); (b) J.-Y. Sun, Ph.D. Thesis, University of North Carolina, 1967.

(24) J. R. Hutchison, J. G. Gordon, II, and R. H. Holm, submitted for publication.

(25) J. T. Adams and C. R. Hauser, *J. Amer. Chem. Soc.*, **66**, 1220 (1944); F. W. Swamer and C. R. Hauser, *ibid.*, **72**, 1352 (1950).

saturated sodium chloride solutions, dried over calcium sulfate, and the ether was removed *in vacuo*. The reddish yellow oil (~80 ml) was dissolved in 120 ml of methanol and added to a solution of 60 g of cupric acetate in 600 ml of hot water. The blue cupric complex was collected by filtration, washed well with water, and decomposed by shaking a suspension of it in 500 ml of ether with 400 ml of 20% sulfuric acid. The yellow ether layer was separated, washed and dried as above, and the ether was removed. Distillation of the remaining yellow oil afforded 34 g (44%) of the colorless β-diketone, bp 66° (21 mm) [lit.[25] bp 66–67° (20 mm)]. The compound was shown to be pure and to consist of >95% enol form by its pmr spectrum (neat): Me(*i*-Pr), −1.10 (J = 7 Hz); Me, −2.00; H(*i*-Pr), −2.42; H(ring), −5.55; OH, −15.6 ppm (enol).

The complex was prepared by adding 15.7 g (0.0434 mol) of sodium tris(carbonato)cobaltate(III) trihydrate[26] to a refluxing solution of 16.7 g (0.130 mol) of 5-methylhexane-2,4-dione in 100 ml of 60% acetone–water (v/v). Concentrated nitric acid (9 ml) was added dropwise down the reflux condenser (*caution*—foaming). After addition was complete the reaction mixture was refluxed for 15 min, cooled, and extracted with ether. The green ether layer was dried over calcium sulfate and the ether removed to afford a green oil, which was then dissolved in 15 ml of *n*-hexane. This solution was applied to a 15 × 5 cm column of Merck acid-washed alumina. *n*-Hexane (100 ml) was passed through the column and the green complex was then rapidly eluted with benzene leaving lavender and brown bands on the column. Removal of the benzene in a rotary evaporator produced ~17 g of a green oil which contained some solvent. Exposure of this material to oil pump vacuum overnight yielded the complex in an adequate state of purity as a green gum which did not crystallize.

Anal. Calcd for $C_{21}H_{33}O_6Co$: C, 57.27; H, 7.55: Found: C, 57.24; H, 7.52.

Separation of Isomers. The *cis* and *trans* isomers were separated completely by chromatography on Merck acid-washed alumina (75–100 g/g of complex) in a 52-mm o.d. tube. The isomeric mixture (4.5 g) dissolved in 10 ml of *n*-hexane was put on the column and eluted with 3:2 *n*-hexane–benzene (v/v). Initial breakthrough of the bands containing the *trans* and *cis* isomers occurred after 2–3 and *ca.* 7 hr, respectively. The total separation time could be decreased by extruding the column under nitrogen pressure after the *cis* and *trans* bands were completely separated (*ca.* 4 hr). The column was divided into sections, each of which was thoroughly extracted with ether or dichloromethane. The upper section yielded pure *cis*, the lower section pure *trans*, and a small intermediate section was discarded owing to some trailing of the *trans* band. Removal of solvent from the extracts of the upper and lower sections gave green oils, which when subjected to oil pump vacuum for several days became sticky green gums. Fractions obtained in this way or by complete elution from the column were shown by their pmr spectra to contain only one isomer. The order of movement on the alumina column, *viz.*, *trans* > *cis*, is the same as that observed previously for other tris(β-diketonato)-metal(III) complexes.[2,3] After several weeks the gums partially crystallized, giving soft crystals with the following approximate melting points: *trans*, 56–58°; *cis*, 57–60°. Pmr and electronic spectral data for the pure isomers are given in Table I. A pmr spectrum of the isomeric mixture is shown in Figure 1.

Partial Resolution of *cis* and *trans* Isomers. A 3.0-cm diameter Pyrex column was packed to a height of 170 cm with D-lactose (Baker analyzed reagent grade), which had been sieved to 100 mesh and dried at 120°. The procedure of Collman, *et al.*, and Sun[23] for packing a lactose column was followed. A solution of 40–50 mg of the *cis* or *trans* isomer in 2–3 ml of *n*-hexane was applied to the column and eluted with *n*-hexane. Breakthrough occurred in about 5 hr. For both the *cis* and *trans* isomers the first fractions showed negative rotations and the last fractions positive rotations at 546 mμ. Data for typical runs (9-ml fractions were collected) follow (fraction number, $[M]_{546}^{25}$ *cis*, $[M]_{546}^{25}$ *trans*): 4, 0.00, −2830; 8, −3540, −210; 12, −250, +760; 16, +900, +2600; 20, +3840, +2970. The extent of resolution indicated by these rotations is adequate for accurate polarimetric measurement of racemization rates of the two isomers. It is, however, very small and may be estimated from the molar rotations of the two enantiomers of completely resolved $Co(acac)_3$.[23b] The average value of $[M]_{546}^{25}$ for the latter is ±29,000 in 1:1 (v/v) benzene–heptane. Taking this value as the limiting rotation for $Co(mhd)_3$, the optical purities of the most active *cis* and *trans* samples are estimated as *ca.* 10%.

(26) H. F. Bauer and W. C. Drinkard, *Inorg. Syn.*, **8**, 202 (1966).

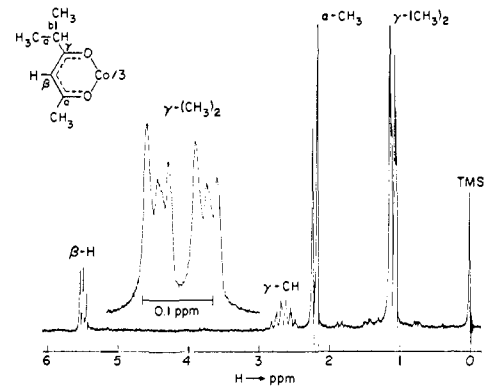

Figure 1. Pmr spectrum (100 MHz) of an equilibrium mixture of *cis*- and *trans*-$Co(mhd)_3$ in $CDCl_3$ solution at *ca.* 30°. Insert: expanded spectrum of the diastereotopic methyl groups (a, b) of the γ-*i*-Pr ring substituent.

Purification of Solvent. Rates of isomerization and racemization of $Co(mhd)_3$ were measured in chlorobenzene solution. The use of this solvent permits direct comparison of these rate data with those of others[19] and polarimetric measurements in commercially available cells up to 105°. Chlorobenzene was purified by washing with concentrated sulfuric acid followed by distillation in which a middle cut with bp 130° (1 atm) was collected. This batch was passed through a silica gel column, redistilled from phosphorus pentoxide, and a second middle cut with the same boiling point collected. Batches obtained in this way were used for preparation of solutions employed in rate measurements.

Table I. Pmr and Electronic Spectral Data for *cis*- and *trans*-$Co(mhd)_3$

Isomer	Chemical shifts,[a] ppm		λ_{max}, cm^{-1}; ε, l. mol^{-1} cm^{-1} [b]
cis	CH_3(*i*-Pr)	−1.049[c]	43,300; 40,500
		−1.081[c]	38,300; 35,000
	CH_3	−2.13	33,900 (sh); 11,400
	CH(*i*-Pr)	−2.59[d]	31,250 (sh); 7210
	CH	−5.46	16,860; 143
trans	CH_3(*i*-Pr)	−1.062[e]	43,300; 40,700
	CH_3	−2.13 (1)	38,300; 35,700
		−2.20 (2)	33,900 (sh); 11,500
	CH(*i*-Pr)	−2.64[d]	31,250 (sh); 7250
	CH	−5.42 (1)	16,840; 142
		−5.51 (2)	

[a] $CDCl_3$ solution, TMS reference. [b] Cyclohexane solution. [c] Center of doublet, J = 6.8 Hz. [d] Center of multiplet, J = 6.8 Hz. [e] Center of complex doublet, J ~ 7 Hz (*cf.* Figure 1).

Measurement of Isomerization Rates. The rates of isomerization of *cis*- and *trans*-$Co(mhd)_3$ were measured in chlorobenzene solution in the interval 90–110°. In a typical kinetic run a sealed nmr tube containing a solution of one isomer was immersed in a constant temperature bath (±0.1°) for the desired period of time, and the isomerization reaction was then quenched by plunging the tube in an ice–methanol bath (*ca.* −15°). The pmr spectrum of the methyl group directly attached to the chelate ring was recorded at least six times at ambient probe temperature on a Varian HR-100 spectrometer. Relative concentrations of the two isomers were determined by comparison of the relative heights of the same peaks in standard solutions of known concentrations. The latter were prepared by volume in nmr tubes (using microliter syringes) from standard stock solutions of the chromatographically pure isomers. The procedure may be understood by reference to Figure 2, which shows time-dependent methyl spectra recorded during a kinetic run at 90° using as the initial isomer pure *trans*. In a freshly prepared solution two methyl peaks of relative intensity 2:1 at −1.95 and −1.93 ppm, respectively, are observed. The signal of the *cis* form at −1.92 ppm is seen to grow in with time. Relative concentrations were obtained from the measured peak height ratios of this signal to the two *trans* signals and the use of a

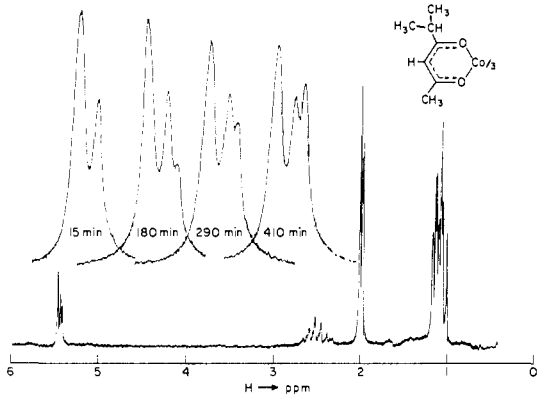

Figure 2. Pmr spectrum (100 MHz) of an equilibrium mixture of *cis*- and *trans*-Co(mhd)$_3$ in chlorobenzene solution at *ca.* 30°. Insert: expanded spectra of the α-CH$_3$ group at various times in an isomerization rate run at 90°; 15 min, nearly pure *trans;* 410 min, equilibrium mixture.

calibration curve, which is most conveniently plotted as log (peak height *trans*/peak height *cis*) *vs.* mole fraction of *cis* or *trans*. Reactions were followed essentially to completion (greater than three half-lives) and five measurements of relative concentrations were made per run. The equilibrium constant was measured at the completion of the reaction. All spectra were recorded at constant power setting (at least 10 db below saturation), and the calibration curve was rechecked on each different day a kinetic run was performed. For the isomerization reaction

$$cis \underset{k_{TC}}{\overset{k_{CT}}{\rightleftharpoons}} trans$$

the rate constants were obtained by use of eq 6 (see later text). Runs were made from both pure *cis* and pure *trans* and the data fit by a least-squares procedure to the appropriate equation. In a given run the rate constant in one direction was determined from the slope and the reverse rate constant calculated from the equilibrium constant. Equilibrium and rate constant data are set out in Table II.

Table II. Rate Constants for Isomerization of Co(mhd)$_3$ in Chlorobenzene Solution

Initial isomer	Temp, °C	$k_{CT} \times 10^5$, sec^{-1} [b]	$k_{TC} \times 10^5$, sec^{-1} [b]	K_{eq} [c]	Concn, M [a]
trans	89.8	5.55	2.75		0.260
cis	90.0	4.94	2.37	2.08	0.427
trans	90.0	6.30	3.22	1.96	0.356
trans	98.9	18.5	8.47	2.18	0.260
cis	100.0	19.1	8.82	2.16	0.427
trans	100.0	21.1	9.72	2.18	0.356
cis	110.0	61.1	29.1	2.10	0.427
trans	110.0	67.6	32.2	2.10	0.356

[a] At *ca.* 25°. [b] The estimated standard deviation as computed for each run from the residuals of the least-squares fitted line vary from 3 to 10%. Consideration of the accuracy of measuring the equilibrium constant and of errors in the determination of the mole fractions of the isomers which may be systematic for a given run leads to an estimate of ±30% as the *maximum* probable error of an individual rate constant. [c] K_{eq} = (*trans*)/(*cis*).

Measurement of Racemization Rates. The rates of racemization of partially resolved *cis*- and *trans*-Co(mhd)$_3$ were measured in chlorobenzene solution in the interval 80–105°. A Perkin-Elmer Model 141 spectropolarimeter and a jacketed cell of length 10 cm and 1-ml capacity attached to a circulating constant-temperature bath (±0.1°) were employed. Partially resolved samples were rechromatographed on Merck acid-washed alumina (benzene eluent), dried for several days *in vacuo*, and solutions were prepared in freshly distilled chlorobenzene. All solutions were manipulated under dry nitrogen and stored in a refrigerator in the dark. Racemization rates were found to be somewhat sensitive to solvent purity and traces of moisture. Optical rotations were measured at 546 mμ with the light beam blanked out between readings in order to avoid any photochemical decomposition such as has been observed for Co(acac)$_3$[27] when exposed to light in the region of ligand-field absorptions. Initial rotations varied from 0.100 to 0.800° and were typically about 0.250°. Concentrations of solutions were measured spectrophotometrically. Kinetic runs were usually carried out over at least two half-lives and the average number of measurements per run was 30. Racemization rate constants k_r were evaluated from the slopes of least-squares plots of ln α_{obsd} *vs.* time. Rate constant data are given in Table III.

Circular Dichroism Spectra. CD measurements of partially resolved *cis*- and *trans*-Co(mhd)$_3$ were made on a Cary Model 60 spectrometer using 1-cm cells and cyclohexane as the solvent.

Results and Discussion

A general formulation of isomerization and racemization kinetics is first given, followed by a comparison of experimentally determined rate constant ratios for Co(mhd)$_3$ with those predicted from consideration of possible twist and bond rupture mechanisms. The notation for absolute configurations, Δ and Λ, is that employed earlier.[28] The isomers *cis*-Λ (CΛ) and *trans*-Λ (TΛ) are illustrated by **2** and **3**, respectively.

2 **3**

Treatment of Kinetics. The four species subject to isomerization and/or racemization are CΔ, CΛ, TΔ, TΛ. Allowing all possible interconversions among these species leads to six rate constants which are defined by the transformations of eq 1. In the general case

$$\begin{aligned}
C\Delta(C\Lambda) &\xrightarrow{k_1} T\Delta(T\Lambda)\\
C\Delta(C\Lambda) &\xrightarrow{k_2} T\Lambda(T\Delta)\\
T\Delta(T\Lambda) &\xrightarrow{k_3} C\Delta(C\Lambda)\\
T\Delta(T\Lambda) &\xrightarrow{k_4} C\Lambda(C\Delta)\\
C\Delta &\underset{}{\overset{k_5}{\rightleftharpoons}} C\Lambda\\
T\Delta &\underset{}{\overset{k_6}{\rightleftharpoons}} T\Lambda
\end{aligned} \qquad (1)$$

where all isomers are present four equations are required to relate explicitly the rate of concentration change of one isomer to the concentrations of all the others. These relations are conveniently expressed by the matrix of eq 2; in this and the following kinetic equations the italicized symbols for the species represent

$$\begin{pmatrix} dC\Delta/dt \\ dC\Lambda/dt \\ dT\Delta/dt \\ dT\Lambda/dt \end{pmatrix} = \begin{pmatrix} -(k_1+k_2+k_5) & k_5 & k_3 & k_4 \\ k_5 & -(k_1+k_2+k_5) & k_4 & k_3 \\ k_1 & k_2 & -(k_3+k_4+k_6) & k_6 \\ k_2 & k_1 & k_6 & -(k_3+k_4+k_6) \end{pmatrix} \begin{pmatrix} C\Delta \\ C\Lambda \\ T\Delta \\ T\Lambda \end{pmatrix} \qquad (2)$$

(27) N. Filipescu and H. Way, *Inorg. Chem.*, **8**, 1863 (1969).
(28) T. S. Piper, *J. Amer. Chem. Soc.*, **83**, 3908 (1961).

Table III. Rate Constants for Racemization of Co(mhd)$_3$ in Chlorobenzene Solution

cis[a]			*trans*[a]		
Temp, °C	$k_r \times 10^5$,[d] sec^{-1}	Concn,[b] $M \times 10^3$	Temp, °C	$k_r \times 10^5$,[d] sec^{-1}	Concn,[b] $M \times 10^3$
80.0	2.96 (3)	[c]	79.9	4.05 (3)	2.08
90.0	10.3 (1)	[c]	85.0	7.79 (3)	1.05
	10.2 (1)	[c]	90.0	15.7 (1)	1.05
	9.92 (6)	[c]		14.2 (1)	2.08
	10.3 (1)	[c]		15.8 (1)	2.08
95.0	16.4 (7)	0.272		16.8 (4)	[c]
	18.3 (1)	0.544	95.0	27.3 (3)	0.695
	17.5 (1)	0.720		26.8 (1)	1.04
	18.0 (1)	1.09		26.4 (1)	1.39
	19.0 (1)	1.44		26.9 (1)	2.09
	17.7 (1)	2.18		27.0 (1)	2.78
100.0	31.0 (2)	1.09	100.0	49.2 (3)	1.05
	33.7 (3)	[c]		50.8 (4)	2.08
105.0	47.4 (3)	1.09			
	54.4 (3)	1.09			
	59.6 (6)	[c]			

[a] Initial isomer. [b] At *ca.* 25°. [c] Concentration not accurately determined but in the range 0.4–0.7 $\times 10^{-3}$ *M*. [d] The errors in parentheses are the standard derivations of the last significant digit estimated from the residuals of the least squares line for each run; the probable error for an individual rate constant is estimated as ±7%.

their concentrations ($T\Delta$ = [$T\Delta$], etc.). When the process of interest is *isomerization*, only the total concentrations of *cis* and *trans* isomers, $C = C\Delta + C\Lambda$ and $T = T\Delta + T\Lambda$, are required. In this case the relevant relationships are given by eq 3. By reference

$$\begin{pmatrix} dC/dt \\ dT/dt \end{pmatrix} = \begin{pmatrix} -(k_1 + k_2) & (k_3 + k_4) \\ (k_1 + k_2) & -(k_3 + k_4) \end{pmatrix} \begin{pmatrix} C \\ T \end{pmatrix} \quad (3)$$

to the isomerization reaction 4 the identifications in eq 5 may be made. The equations represented by eq 3

$$C \underset{k_{TC}}{\overset{k_{CT}}{\rightleftharpoons}} T \quad (4)$$

$$k_{CT} = k_1 + k_2 \qquad k_{TC} = k_3 + k_4 \quad (5)$$

may be solved explicitly to give the following rate relation, expressed in terms of mole fraction of the *cis* isomer and k_{CT}.

$$\ln [N_C(1 + K_{eq}) - 1] = -k_{CT}\left(\frac{1 + K_{eq}}{K_{eq}}\right)t + \ln [N_C^0(1 + K_{eq}) - 1] \quad (6)$$

In eq 6 N_C and N_C^0 are the mole fractions of *cis* at time t and $t = 0$, respectively, and $K_{eq} = N_T/N_C = k_{CT}/k_{TC}$. The rate constant k_{CT} may be obtained from a plot of ln [$N_C(1 + K_{eq}) - 1$] *vs.* t and thereafter k_{TC} evaluated.

In a *racemization* reaction the observed optical rotation is proportional to the differences in concentrations of the Δ and Λ enantiomers of each isomer, *i.e.*, to C', T', or $C' + T'$ where $C' = C\Delta - C\Lambda$ and $T' = T\Delta - T\Lambda$. The appropriate equations are then given by

$$\begin{pmatrix} dC'/dt \\ dT'/dt \end{pmatrix} = \begin{pmatrix} -(k_1 + k_2 + 2k_5) & (k_3 - k_4) \\ (k_1 - k_2) & -(k_3 + k_4 + 2k_6) \end{pmatrix} \begin{pmatrix} C' \\ T' \end{pmatrix} \quad (7)$$

A general solution to this set of equations is algebraically cumbersome. Therefore, solutions will be obtained for specific reaction pathways considered in subsequent sections.

Experimental Isomerization and Racemization Rates. The pmr spectra of an equilibrium mixture of Co(mhd)$_3$ isomers in chloroform and chlorobenzene solutions are shown in Figures 1 and 2, respectively. The expanded spectrum in the isopropyl methyl region (Figure 1) is of interest for it reveals three methyl doublets; two such doublets (*cf.* Table I) are observable in the spectrum of the pure *cis* isomer. Because of the chirality of both isomers methyl groups therein are diastereotopic. In this case components of three of the eight methyl doublets whose chemical shifts are in principle different can be resolved. Observation of diastereotopic effects in chiral metal chelates is relatively rare;[29] these effects are being utilized in our studies[24] of the rearrangement reactions of fast complexes. Isomerization rates of *cis*- and *trans*-Co(mhd)$_3$ in chlorobenzene were determined by measurement of α-CH_3 proton signal intensities as a function of time (*cf.* Figure 2). Rate constants are presented in Table II. k_{CT} was calculated directly from the intensity data and k_{TC} was obtained from k_{CT} and the equilibrium constant. The estimated maximum probable error of ±30% in the rate constants arises mainly from the error in measuring N_C and the resulting error (±5–10%) in K_{eq}. The estimated standard deviations of individual rate constants, as calculated from least-squares fit to eq 6, are smaller (3–10%), but these neglect the error in K_{eq}. The isomerization reaction is considered first order because kinetic plots show no curvature and the measured rates do not appear to be concentration dependent outside of experimental uncertainty. However, the inherent sensitivity of measurements of relative concentrations by pmr did not permit solutions less concentrated than *ca.* 0.20 *M* to be studied accurately.

Racemization rates of *cis*- and *trans*-Co(mhd)$_3$ were determined polarimetrically in chlorobenzene and rate constants are set out in Table III. The estimated maximum probable error in the rate constants is ±7%.

(29) For particularly clear examples of magnetic nonequivalence due to molecular chirality in metal complexes, *cf.* L. H. Pignolet and R. H. Holm, *J. Amer. Chem. Soc.*, **92**, 1791 (1970). Note also that the complex methyl signals in *trans*-tris(N-isopropylpyrrole-2-aldiminato)cobalt(III) may be a consequence of the diastereotopism of the methyl groups: A. Chakravorty and R. H. Holm, *Inorg. Chem.*, **3**, 1521 (1964).

Table IV. Kinetic Parameters for the Intramolecular Rearrangements of $Co(mhd)_3$ and Related Complexes in Chlorobenzene Solution

Process	Rate constant, sec^{-1}, 90°	Ln A, sec^{-1}	E_a, kcal mol^{-1}	$\Delta H^{\ddagger}$, kcal mol^{-1}	$\Delta S^{\ddagger}$, eu
Isomerization: $Co(mhd)_3$					
cis → *trans*	k_{CT} $5.75 \pm 1.70 \times 10^{-5}$	35.8 ± 1.9	32.9 ± 1.4	32.9 ± 1.1	8.7 ± 2.9
trans → *cis*	k_{TC} $2.75 \pm 0.80 \times 10^{-5}$	34.6 ± 2.2	32.6 ± 1.6	32.6 ± 1.4	6.3 ± 3.9
Racemization: $Co(mhd)_3$					
cis[a]	k_{rC} $1.00 \pm 0.07 \times 10^{-4}$	33.1 ± 0.8	30.5 ± 0.6	29.9 ± 0.6	1.5 ± 1.6
trans	k_{rT} $1.50 \pm 0.10 \times 10^{-4}$	36.4 ± 1.1	32.6 ± 0.8	31.6 ± 0.7	6.8 ± 1.8
Isomerization: $Co(tfac)_3$[b]	k_{CT} $5.20 \pm 0.16 \times 10^{-4}$	35.0 ± 0.8	30.7 ± 0.6		8.6 ± 1.7
	k_{TC} $1.3 \pm 0.1 \times 10^{-4}$				
Linkage isomerization[c]					
$Co(triac\text{-}d_3)_3$	k_i 3.0×10^{-5}		39.3 ± 3.8		
$Co(triac\text{-}d_3)(acac)_2$	k_i 2.5×10^{-5}				
Racemization[c]					
$Co(acac)_3$	k_r 8×10^{-5}				
$Co(triac\text{-}d_3)(acac)_2$	k_r 4.2×10^{-4}				
$Co(triac\text{-}d_3)_3$	k_r 9.4×10^{-4}		31.0 ± 1.3		

[a] Initial isomer. [b] Data from ref 11, chloroform solution. [c] Data from ref 19.

First-order kinetics is indicated by the lack of curvature in the kinetic plots and of systematic dependence of rate on concentration in the multiple measurements of the two isomers at 95°.

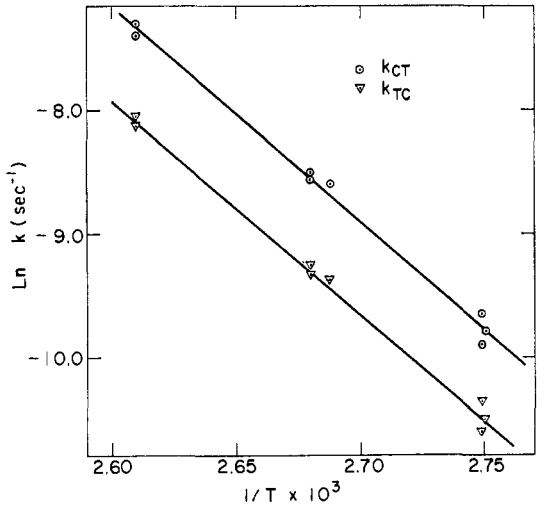

Figure 3. Arrhenius plot for the isomerization of *cis*- and *trans*-$Co(mhd)_3$ in chlorobenzene solution over the range 90–110°.

Arrhenius plots for isomerization and racemization of each isomer are displayed in Figures 3 and 4, respectively. Activation energies (E_a) and preexponential factors (A), as well as enthalpy and entropy changes of activation, calculated assuming the Eyring equation (eq 8) is valid, are given in Table IV for the two processes. The indicated errors are one standard de-

$$k = \frac{RT}{Nh} \exp(-\Delta H^{\ddagger}/RT) \exp(\Delta S^{\ddagger}/R) \qquad (8)$$

viation estimated from least-squares fits to the appropriate equations. Rate constants at 90° were obtained from the Arrhenius plots. The rates of isomerization and racemization are of the same order of magnitude and activation energies and enthalpy changes for the two reactions of either isomer agree to within several kilocalories/mole. On the basis of these data it is highly probable that both reactions proceed through the *same* transition state, the nature of which is investigated in following sections.

The isomerization reaction was further studied in order to learn whether or not it took place with any degree of stereoselectivity. Partially resolved, pure *cis*- or *trans*-$Co(mhd)_3$ was heated in chlorobenzene for a time short compared to the isomerization half-life, the resultant isomeric mixture separated by tlc,

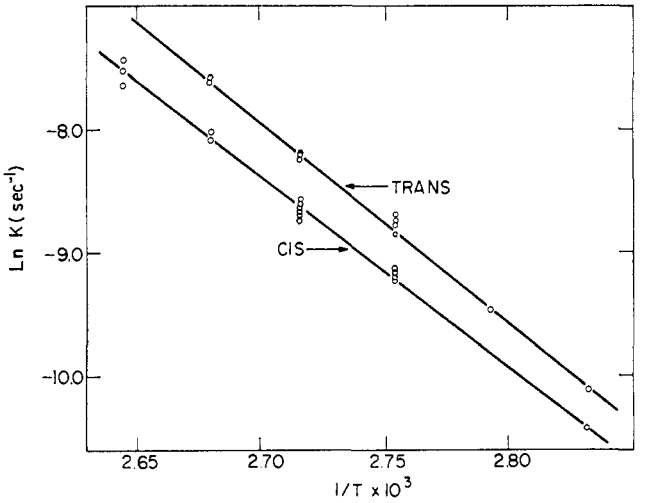

Figure 4. Arrhenius plot for the racemization of *cis*- and *trans*-$Co(mhd)_3$ in chlorobenzene solution over the range 80–105°.

and the rotation of each isomer measured. The results of several such experiments are shown in Table V. If the entirely reasonable assumption is made that a given configuration of *cis* and *trans* has the same sign of rotation, the data show qualitatively that *isomerization occurs with inversion of configuration.*

The ratio of the limiting rotations of the *cis* and *trans* isomers and values of the microscopic rate constants may be estimated by the following procedure, in which $[M]^t$ is molar rotation at time t and $[M^0]$ the molar rotation of a completely resolved isomer. From these definitions it follows that

$$[M_C]^t = \frac{C'}{C}[M_C{}^0] \qquad [M_T]^t = \frac{T'}{T}[M_T{}^0] \qquad (9)$$

If an experiment is conducted starting with, *e.g.*, pure, partially resolved *cis*, and allowed to proceed for a short time, the back reactions of *trans* can be neglected

Table V. Evidence for Configurational Inversion in the Isomerization of *cis*- and *trans*-Co(mhd)$_3$ in Chlorobenzene[a]

Initial isomer	Initial $[M]_{546} \times 10^{-2}$	Reaction time[b] at 95°, min	Obsd $[M]_{546} \times 10^{-2}$ *cis*[c]	Obsd $[M]_{546} \times 10^{-2}$ *trans*[c]
cis	−38.7 ± 1.2	20	−39.6 ± 1.2	+29.2 ± 1.5
cis	−38.7 ± 1.2	20	−38.7 ± 1.2	+29.4 ± 1.5
			av −39.2 ± 1.2	+29.3 ± 1.5
cis	−38.7 ± 1.2	40	−35.2 ± 1.4	+26.3 ± 1.0
trans	+17.6 ± 0.7	20	−14.7 ± 1.2	+14.1 ± 0.6
trans	+15.8 ± 0.5	23	−13.0 ± 1.7	+12.4 ± 0.5

[a] Rotations measured at ~25°. [b] 20 min corresponds to $\sim 0.28 t_{1/2}$ for isomerization. [c] Separated by tlc (Mallinckrodt Chrom-AR 500, silica gel, chloroform eluent); concentrations measured spectrophotometrically.

and it is readily seen from eq 7 that

$$\frac{dT'}{dt} \approx (k_1 - k_2)C' = (k_1 - k_2)C[M_C]^t/[M_C{}^0] \quad (10)$$

Under these circumstances $C \approx C_0 \exp(-k_{CT}t) = C_0 \exp[-(k_1 + k_2)t]$ and $[M_C]^t$ can be assumed to be essentially constant and equal to the initial rotation $[M_C]^0$. Therefore

$$T' \approx \frac{(k_1 - k_2)C_0(1 - \exp[-(k_1 + k_2)t])}{(k_1 + k_2)} \frac{[M_C]^0}{[M_C{}^0]} \quad (11)$$

Because $T = C_0 - C \approx C_0(1 - \exp[-(k_1 + k_2)t])$, it follows that

$$\frac{[M_C{}^0]\,[M_T]^t}{[M_T{}^0]\,[M_C]^0} \approx \frac{(k_1 - k_2)}{(k_1 + k_2)} \quad (12a)$$

If the initial isomer is pure, partially resolved *trans*, an analogous treatment yields the relationship in eq 12b. Of the four rate constants in eq 12, only three

$$\frac{[M_T{}^0]\,[M_C]^t}{[M_C{}^0]\,[M_T]^0} \approx \frac{(k_3 - k_4)}{(k_3 + k_4)} \quad (12b)$$

are independent, since $k_1/k_2 = k_3/k_4$. Substitution of the data in Table V for $t = 20$ min into these equations yields the following results

$$\frac{[M_C{}^0]}{[M_T{}^0]} = 1.05 \pm 0.05 \qquad \frac{k_2}{k_1} = \frac{k_4}{k_3} = 8.8 \pm 1.9$$

$$k_1 = 1.1 \pm 0.4 \times 10^{-5}\ \text{sec}^{-1}$$

$$k_2 = 9.6 \pm 3.5 \times 10^{-5}\ \text{sec}^{-1}$$

$$k_3 = 0.52 \pm 0.17 \times 10^{-5}\ \text{sec}^{-1}$$

$$k_4 = 4.6 \pm 1.7 \times 10^{-5}\ \text{sec}^{-1}$$

That the ratio of limiting molar rotations is very close to unity is highly reasonable inasmuch as the rotational strength of a complex such as **1** should depend nearly completely on its chirality alone, especially in the d–d region where experimental rotations are recorded. In the analysis of mechanisms which follows, use will be made of the rate constant ratios. These are independent of the measurement of the overall isomerization rate constants k_{CT} and k_{TC}, whereas k_1–k_4 were calculated using these constants.

Maximum values of k_5 and k_6 can be estimated from the data in Table V and were found to be 4×10^{-5} and 16×10^{-5} sec^{-1}, respectively. However, more accurate values of these rate constants were obtained from eq 7. Using the computer program described in the followng sections, racemization rates were calculated for varying values of k_5 and k_6 and the above values of k_1–k_4. Comparison of these rates with those observed at 95° yielded the following values: $k_5 \sim 0$ and $k_6 = 8.6 \pm 0.8 \times 10^{-5}$ sec^{-1}.

Reaction Pathways. (a) Twist Mechanisms. Isomerization and racemization reactions proceeding by a non-bond-breaking mechanism may be most easily visualized by twist motions of the three chelate rings about axes bisecting opposite triangular faces of the coordination octahedron.[12,16] Unsymmetrical bidentate ligands permit a true or real C_3 axis only in the *cis* isomer. However, such axes, whether rigorous symmetry elements or not, are the most useful geometrical constructs with respect to which ring motions may be referred. Adopting the definitions of Springer and Sievers,[12] these axes are denoted as real (r), pseudo (p), and imaginary (i). Rotations about any of the six distinguishable axes (two for *cis* and four for *trans*) by 60° produces transition states with effective trigonal prismatic symmetry. The types of axes and ring mo-

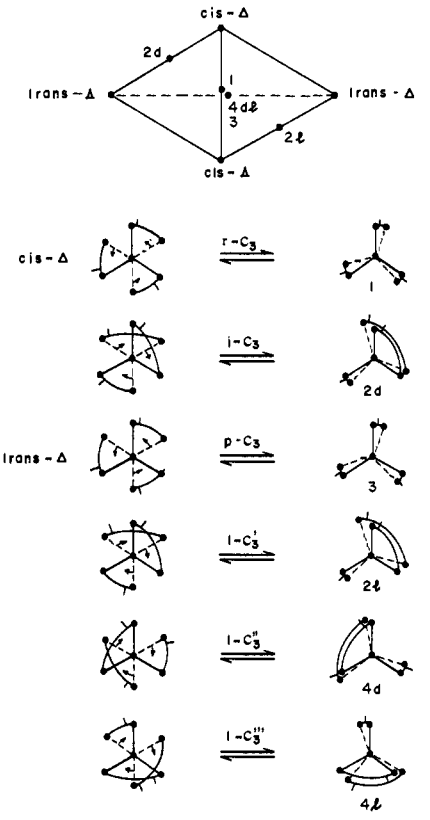

Figure 5. Topological correlation diagram for the interconversion of isomers by twist mechanisms. The six possible trigonal-prismatic transition states produced by ring motion relative to the real (r), pseudo (p), and imaginary (i) threefold axes are illustrated.

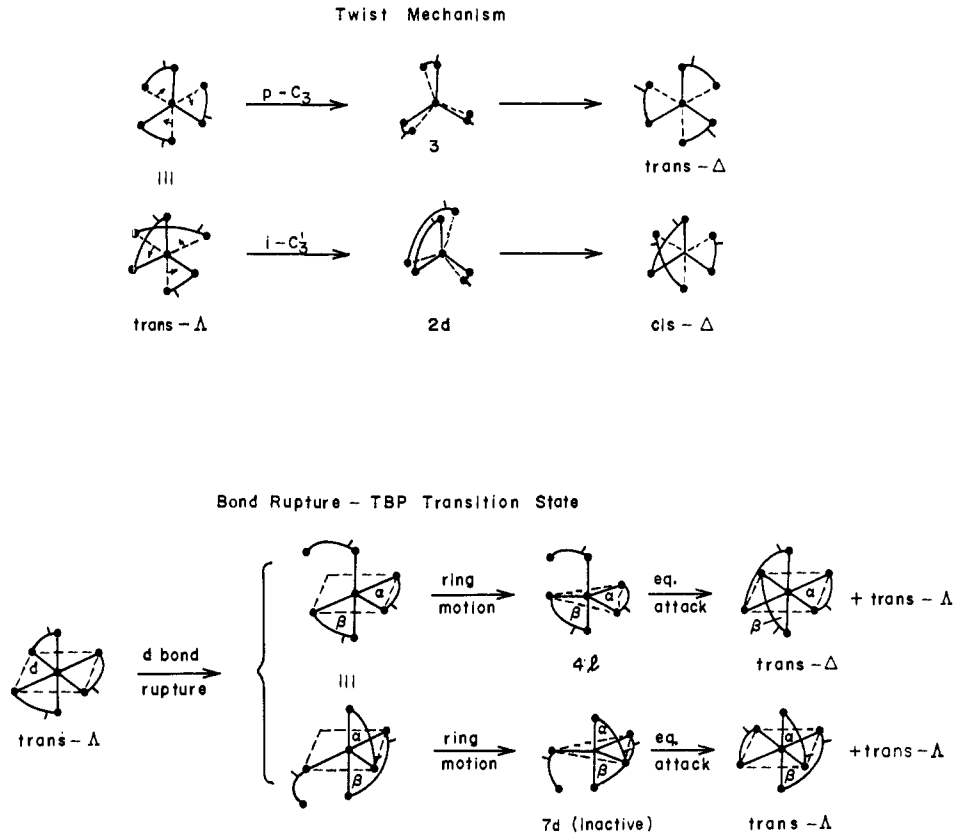

Figure 6. Illustration of the formation of products in reactions of *trans*-Λ proceeding by the twist and bond-rupture mechanisms. TBP transition states **4***l* and **7***d* possess dangling axial and equatorial ligands, respectively. α and β designate chelate ring planes which have different relative orientations in the two types of TBP transition states.

tions which produce the six possible transition states for *cis*- and *trans*-Δ are illustrated in Figure 5. Continued rotation past the transition state generates the rearrangement product, as shown in Figure 6 for twist motions around p-C_3 and one i-C_3 axis of *trans*-Λ. All possible interconversions proceeding through the six transition states are summarized by the correlation diagram[14,30] at the top of Figure 5. Note that all interconversions occur with *inversion* of configuration and thus k_1 and $k_3 = 0$. The remaining rate constants may be nonzero. Because both *cis*- and *trans*-Co(mhd)$_3$ undergo simultaneous isomerization and racemization, twists about the r- and p-C_3 axes alone are eliminated.

The connection between the consequences of the various possible twist operations and the observed isomerization and racemization rates can be made through the microscopic rate constants for the transformations of eq 1. Defining k_c and k_t as the rates at which the *cis* and *trans* isomers, respectively, produce some transition state, the generalized eq 13 may be

$$\begin{aligned} k_1 &= 0 & k_3 &= 0 \\ k_2 &= 3R_i k_c/2 & k_4 &= R_i' k_t/2 \\ k_{CT} &= 3R_i k_c/2 & k_{TC} &= R_i' k_t/2 \\ k_5 &= R_r k_c/2 \\ k_6 &= (R_p + R_i'' + R_i''')k_t/2 \end{aligned} \qquad (13)$$

written in terms of the probabilities R of ring motion about the different axes. $R_r + 3R_i = 1$ for *cis* and $R_p + R_i' + R_i'' + R_i''' = 1$ for *trans*. Deviation from a statistical equilibrium distribution of isomers is assumed to be due to differences in the rates at which *cis* and *trans* go to transition states, *i.e.*, to differences in k_c and k_t. Consequently

$$\frac{k_c}{k_t} = \frac{R_i'}{3R_i} K_{eq} \qquad (14)$$

In order to avoid excessive parameterization, twisting motions about axes producing transition states of closely related structures[31] (*cf.* Figure 5) have been given equal probabilities. All R_i in *trans* were assumed to be the same and to be identical with the three necessarily equal R_i values of *cis*; this requires $R_p = R_r$. The value assigned to k_t was such as to make rate constants of the same order of magnitude as the measured racemization rate constants, and k_1–k_6 were calculated[32] as the probability of twist motion about the real (*cis*) and pseudo (*trans*) axes was varied from 0 to 1 in steps of 0.1.

Values of the microscopic rate constants were substituted into eq 7. Because $(k_1 - k_2)$, $(k_3 - k_4) \neq 0$ the solutions to this equation are sums of two ex-

(30) For other topological representations and a matrix description of intramolecular rearrangements of tris chelates by twist mechanisms, *cf.* M. Gielen and C. Depasse-Delit, *Theor. Chim. Acta*, **14**, 212 (1969); M. Gielen, G. Mayence, and J. Topart, *J. Organometal. Chem.*, **18**, 1 (1969); M. Gielen and J. Topart, *ibid.*, **18**, 7 (1969).

(31) Relationships among the various transition states shown in Figure 5 are more clearly evident when considered in the trigonal prismatic perspective illustrated in ref 14.

(32) If, for example, k_t is taken as unity and K_{eq} is given the average experimental value of 2.1 (Table II), then from eq 14, $k_c = 0.7$ and the following expressions for the rate constants in eq 13 are obtained: $k_2 = 0.35(1 - x)$, $k_4 = (1 - x)/6$, $k_5 = 0.35x$, and $k_6 = (x + 2)/6$, where $x = R_p = R_r$.

Table VI. Comparison of Experimental Isomerization and Racemization Rates with Predicted Values[a] for a Twist Mechanism

Rate ratio	R_r or R_p 0.0	0.1	0.2	0.25	0.30	0.40	0.50	Exptl 95°
k_{CT}/k_{rC}	0.603	0.529	0.460	0.426	0.394	0.331	0.270	0.60 ± 0.18
k_{TC}/k_{rT}	0.152	0.138	0.124	0.117	0.110	0.095	0.080	0.19 ± 0.06

[a] Calculated with $R_i(cis) = R_i' = R_i'' = R_i'''(trans)$, $R_r = R_p$, $K_{eq} = 2.1$, $[M_C^0]/[M_T^0] = 1.05$.

ponentials and have the general forms (15). The ex-

$$C' = A_1 \exp(\lambda_1 t) + B_1 \exp(\lambda_2 t)$$
$$T' = A_2 \exp(\lambda_1 t) + B_2 \exp(\lambda_2 t) \quad (15)$$

perimentally measured rotation is proportional to $([M_C^0]C' + [M_T^0]T')$, and, because this quantity is not a simple exponential, a plot of ln α *vs.* t should not be a straight line if some twist mechanism operates. No curvature has been detected in kinetic plots for either isomer. In order to test whether or not a mechanism which should introduce curvature is experimentally distinguishable from a straight line, values of $([M_C^0]C' + [M_T^0]T')$ were calculated as a function of time for each set of microscopic rate constants and a straight line was fit by least squares to a plot of the logarithm of this quantity *vs.* t.[33] Although plots with R_p or $R_r < 20\%$ showed curvature, the esd's of the least-squares lines were smaller than the esd's of the experimental plots. Despite the fact that $k_2 \neq k_1$ and $k_3 \neq k_4$ require two term exponential solutions of eq 7 and consequent curvature in plots of ln α *vs.* t, the degree of curvature expected from twist mechanisms would be obscured by experimental scatter.

A second and more sensitive test of the existence of a twist mechanism has been made from a comparison of experimental and predicted ratios of rate constants. Microscopic rate constants were calculated for different probabilities of rotation about i-C_3 compared to r-C_3 and p-C_3 axes. From these, predicted isomerization rate constants were obtained from eq 5 and predicted racemization rate constants from the plots described above. The results are shown in Table VI. The experimental rate ratios are those at 95°, which is approximately the center of the temperature range of kinetic measurements. Using this treatment the experimental rate ratios agree best with no rotation about the r-C_3 or p-C_3 axes, and are inconsistent with a twist mechanism which proceeds to an extent greater than *ca.* 25% around these axes. However, the ratios k_2/k_1 and k_4/k_3 show that k_1 and k_3 are different from zero. On this basis a twist mechanism may be excluded as the sole reaction pathway.

(b) Bond-Rupture Mechanisms. The relevant mechanisms of this sort can be classified according to the idealized geometry of the transition state—trigonal bipyramidal or square pyramidal. The consequences of these transition states on relative isomerization and racemization rates are considered next.

(i) **TBP Transition States.** Shown in Figure 7 are the TBP transition states produced by breaking in turn the eight distinguishable metal–ligand bonds of *cis*- and *trans*-Λ. All configurations are dissymmetric and may be classified in terms of dangling axial or equatorial ligands. Attack by the end of the dangling ligand affords the initial species or product except

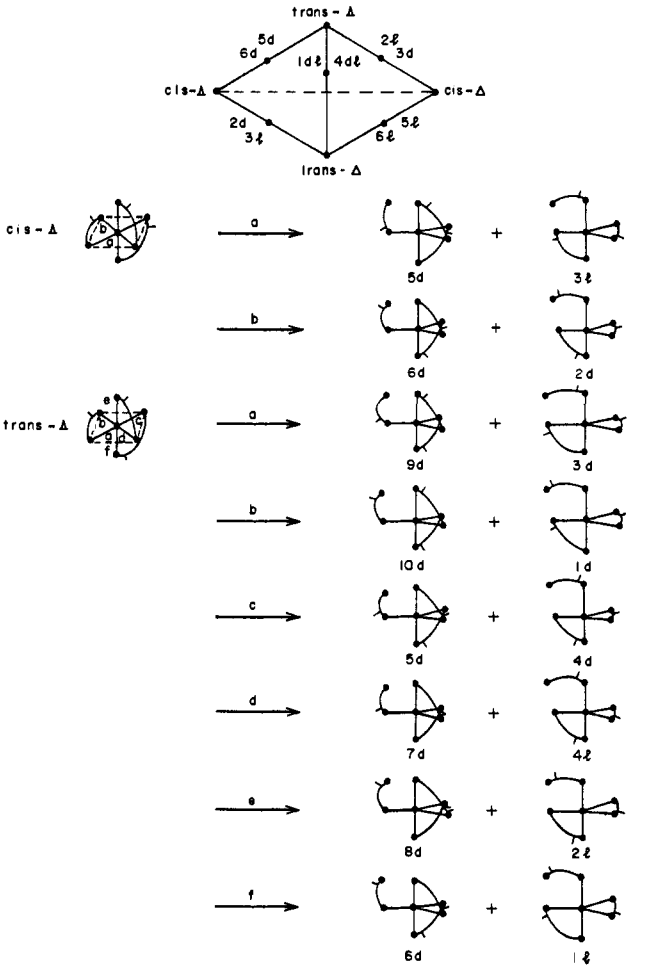

Figure 7. Topological correlation diagram for the interconversion of isomers through TBP transition states. The transition states produced by rupture of the eight distinguishable metal–ligand bonds of *cis*- and *trans*-Λ are shown.

for configurations **7**, **8**, **9**, and **10**, from which only the initial species may be recovered. These transition states with dangling axial and equatorial ligands proceed to products with *inversion* and *retention* of configuration, respectively. The formation of transition states may be visualized by the scheme shown in Figure 6 for a typical bond rupture, that of bond d in *trans*-Λ. The initial entities with vacant octahedral coordination positions are included only for the purpose of indicating how the breaking of any one bond can lead to TBP transition states with dangling axial and equatorial ligands, and are otherwise without physical

(33) A computer program was written which accepted sets of values for k_1–k_6 for the desired probability conditions and produced solutions to eq 7. In the calculations $[M_C^0]/[M_T^0]$ was taken as 1.05 and initial conditions were chosen to give a starting rotation of about 0.5° for both *cis* and *trans*. Plots of ln α *vs.* t and parameters of the best straight lines were obtained as output. Each calculation involved 30 points and about 2 half-lives in order to be statistically comparable to the experimental kinetic plots for racemization.

Table VII. Comparison of Experimental Isomerization and Racemization Rates with Predicted Values[a] for a Bond-Rupture Mechanism and Trigonal-Bipyramidal Transition States

Rate ratio	Probability of TBP-axial transition state						Exptl 95°
	1.00	0.90	0.80	0.70	0.60	0.50	
k_{CT}/k_{rC}	0.584	0.628	0.684	0.758	0.858	1.00	0.60 ± 0.18
k_{TC}/k_{rT}	0.155	0.176	0.200	0.232	0.275	0.333	0.19 ± 0.06

[a] Calculated with $K_{eq} = 2.1$, $[M_C^0]/[M_T^0] = 1.05$.

significance. The diagram at the top of Figure 7 summarizes the possible interconversions of isomers through the twelve active TBP transition states.[34]

values of the microscopic rate constants immediately eliminate a pure TBP-equatorial or a pure TBP-axial mechanism, but are not necessarily inconsistent with a

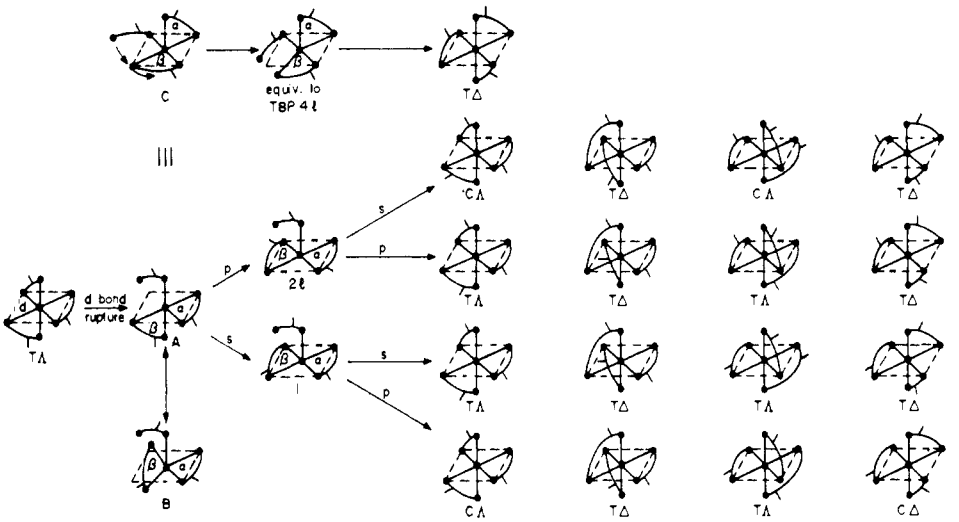

Figure 8. Illustration of the creation of SP-axial transition states (**2*l***, **1**) and formation of products following from the rupture of bond d in *trans*-Λ; p, primary process; s, secondary process. The upper portion shows the equivalence of the SP-basal transition state C and the TBP-axial transition state **4*l***.

Microscopic rate constants for reactions proceeding through the two types of TBP transition states are given by eq 16

TBP-axial	TBP-equatorial
$k_1 = 0$	$k_1 = \frac{1}{2}k_c = k_{CT}$
$k_2 = \frac{1}{2}k_c = k_{CT}$	$k_2 = 0$
$k_3 = 0$	$k_3 = \frac{1}{6}k_t = k_{TC}$ (16)
$k_4 = \frac{1}{6}k_t = k_{TC}$	$k_4 = 0$
$k_5 = 0$	$k_5 = 0$
$k_6 = \frac{1}{3}k_t$	$k_6 = 0$

where k_c and k_t are the rate constants for the formation of transition states from *cis* and *trans*, respectively. Implicit in the specification of rate constants is the assumption that transition states of the same type arising from each isomer are equally probable. Experimental mixed axial–equatorial mechanism. Adopting a procedure entirely analogous to that employed in the investigation of twist mechanisms, predicted racemization rates were obtained from solutions to eq 7, which was solved for sets of k_1–k_6 values representing various combinations of axial and equatorial transition states.[35] Isomerization rate constants were obtained from eq 5 and were suitably weighted. Rate ratios for 50–100% involvement of TBP-axial transition states are given in Table VII. The experimental results are in good agreement with *ca.* 90% TBP-axial involvement, and exclude any combination containing less than *ca.* 70% axial transition states. Further, the measured ratios k_2/k_1 or k_4/k_3 indicate that about 90% of TBP-axial transition states is involved.

(ii) **SP Transition States.** Metal–ligand bond rupture can lead to SP transition states with the dangling ligand in an axial or basal position, as exemplified in Figure 8 by the breaking of bond d in *trans*-Λ. Close examination of the basal species C shows it to be equivalent as a transition state to TBP **4*l***. Attack of the dangling end in the basal plane forces ring β out of this plane, generates a geometry which is very similar to TBP **4*l***, and yields *trans*-Δ as the reaction product. Every SP-basal transition state is equivalent

(34) The transition states given in this figure are labeled identically with those set out by Muettertles.[14] The relationship between his designations of absolute configurations and those used here are $d \equiv \Lambda$ and $l \equiv \Delta$. Note that the topological diagram in Figure 5 of ref 14 incorrectly shows that the interconversions TΔ ⇌ CΔ and TΛ ⇌ CΛ can proceed through transition states **5*d*** and **5*l***, respectively.

(35) Because $k_2 \neq k_1$ and $k_3 \neq k_4$ kinetic plots should be nonlinear, as was the case for twist mechanisms. Analysis of the expected curvatures for the combinations in Table VII indicated that they would be obscured by experimental uncertainty.

in this way to one TBP-axial transition state. Consequently, no kinetic distinction can be made between them and the treatment of the latter given in the preceding section is completely applicable to the SP-basal case.

Visualization of the formation of SP-axial transition states is less straightforward and, as in all mechanistic considerations, requires careful attention to the principle of microscopic reversibility. In the example shown in Figure 8 the ligand β may move in two ways after initial bond breaking to form transition states **2***l* and **1**. The motion which results in the formation of **2***l* is called the primary or p process. It involves rotation of the end of ligand β *trans* to the dangling ligand into the vacant coordination position. Formation of **1** may be formally visualized as rotation of ligand β through *ca.* 90° as it moves to occupy the vacant position. This motion is referred to as the secondary or s process. The primary and secondary transition states generated by breaking the eight distinguishable bonds of *cis*- and *trans*-Λ are shown in Figure 9. Formation of products may be considered to occur by concerted attack of the dangling end at any one of the four positions in the basal plane, and displacement of the appropriate end of a basal ligand to the vacant coordination site below the plane without (p process) or with (s process) rotation of the entire ligand. Because **1** can be obtained from *trans*-Λ by both p and s processes through the breaking of appropriate bonds, it is considered realistic to form products from this transition state by both processes.[36] The products obtained in this way are illustrated in Figure 8. If one process is considered more likely than the other, this difference must be taken into account both in the formation of transition states and in their conversion to products. The correlation diagram in Figure 9 shows the interconversions between isomers which are possible through the agency of SP-axial transition states obtained by both p and s processes. Primary transition states are underlined. Note that all possible interconversions are allowed by means of transition states arising from the p process.

Isomerization and racemization rate constants for reactions proceeding through transition states arising from the microscopic rate constants given by eq 17. k_c

$$k_1 = \frac{1}{4}k_c \qquad k_3 = \frac{1}{12}k_t \qquad k_5 = \frac{1}{4}k_c$$
$$k_2 = \frac{1}{4}k_c \qquad k_4 = \frac{1}{12}k_t \qquad k_6 = \frac{5}{12}k_t \tag{17}$$
$$k_{CT} = \frac{1}{2}k_c \qquad k_{rC} = k_c$$
$$k_{TC} = \frac{1}{6}k_t \qquad k_{rT} = k_t$$

and k_t are the rate constants for formation of transition states from *cis* and *trans*, respectively. These expressions include the assumptions that rupture of all six bonds of initial complex is equally probable and attack by the end of the dangling ligand at all four basal positions in any transition state is also equally probable. Although the predicted rate ratios, $k_{CT}/k_{rC} = 0.5$ and $k_{TC}/k_{rT} = 0.167$, fit experimental results satisfactorily (*cf.* Table VII), the primary process may be excluded as the sole mechanism of isomerization and racemization because it requires $k_1 = k_2$ and $k_3 = k_4$, which is contrary to experiment.

The correlation diagram for interconversions *via* transition states produced by the secondary process alone is given below.

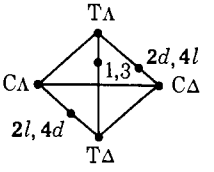

It should be observed that the correlation diagram in Figure 9 is not a simple sum of those for the p and s processes operating separately. The diagram for the latter process immediately reveals that $k_1 = k_3 = 0$, which is consistent with $k_1 < k_2$ and $k_3 < k_4$ found experimentally. In order to make the kinetic treatment more general, formation of transition states by p and s processes is allowed to occur simultaneously

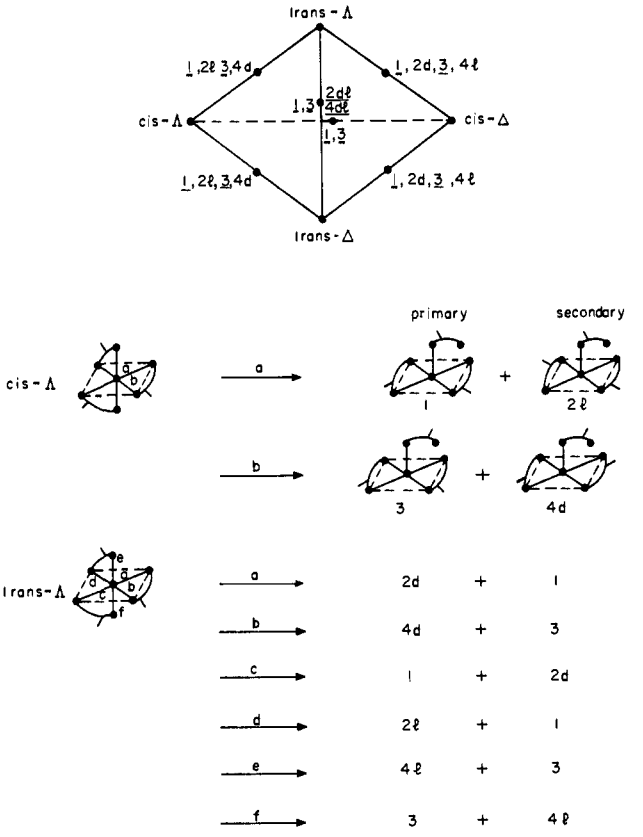

Figure 9. Topological correlation diagram for the interconversion of isomers through SP-axial transition states. The transition states derived from rupture of the eight distinguishable metal-ligand bonds of *cis*- and *trans*-Λ and formed by primary and secondary processes are illustrated. The diagram includes all interconversions following from creation of transition states and their decay to products by both primary and secondary processes. Transition states underlined are formed by the primary process.

(36) The formation of products by *both* processes is not required by microscopic reversibility, but is considered physically reasonable. In the example in Figure 8, reversibility requires only that products be formed from **2***l* and **1** by p and s processes, respectively. In their discussion of SP-axial transition states, Fortman and Sievers[13] allow formation of transiton states by both processes but violate microscopic reversibility by permitting their decay to products only by the p process (*cf.* Figure 5 of ref 13).

Table VIII. Comparison of Experimental Isomerization and Racemization Rates with Predicted Values[a] for a Bond-Rupture Mechanism and Square-Pyramidal-Axial Transition States

Rate ratio	Probability of secondary process 1.00	0.90	0.80	0.70	0.60	0.50	Exptl 95°
k_{CT}/k_{rC}	0.584	0.654	0.709	0.746	0.766	0.768	0.60 ± 0.18
k_{TC}/k_{rT}	0.155	0.188	0.213	0.232	0.243	0.248	0.19 ± 0.06

[a] Calculated with $K_{eq} = 2.1$, $[M_C^0]/[M_T^0] = 1.05$.

Table IX. Comparison of Experimental Isomerization and Racemization Rates with Predicted Values[a] for a Bond-Rupture Mechanism with Mixed TBP-axial and SP-axial Transition States

Rate ratio	Probability of TBP-axial 1.00	0.80	0.60	0.40	0.20	0.00	Exptl 95°
k_{CT}/k_{rC}	0.584	0.618	0.654	0.691	0.729	0.768	0.60 ± 0.18
k_{TC}/k_{rT}	0.155	0.174	0.193	0.211	0.229	0.248	0.19 ± 0.06

[a] Calculated with $K_{eq} = 2.1$, $[M_C^0]/[M_T^0] = 1.05$.

and the ratios of the two are varied. Given in eq 18 are the microscopic rate constants as a function of the fraction y of s process taking place. Predicted racemization rates were obtained from solutions to eq 7 which was solved for sets of k_1–k_6 with different

$$k_1 = \frac{1}{4}(1 + 2y - 3y^2)k_c \qquad k_4 = \frac{1}{12}(1 + 2y - y^2)k_t$$

$$k_2 = \frac{1}{4}(1 + 2y - y^2)k_c \qquad k_5 = \frac{1}{4}(1 - 2y + y^2)k_c$$

$$k_3 = \frac{1}{12}(1 + 2y - 3y^2)k_t \qquad k_6 = \frac{1}{12}(5 - 2y + y^2)k_t \tag{18}$$

$$k_{CT} = \frac{1}{2}(1 + 2y - 2y^2)k_c$$

$$k_{TC} = \frac{1}{6}(1 + 2y - 2y^2)k_t$$

values of y. Predicted isomerization rates were derived from the indicated equations with the same values of y. Rate ratios are given in Table VIII. The best fit with the experimental data occurs with a relatively high proportion of s process. Use of the experimental ratios k_1/k_2 or k_3/k_4 requires that $y \cong 0.9$.

This analysis of the kinetics of isomerization and racemization reactions proceeding through SP-axial transition states leads to definite exclusion of the primary process, and requires production of these transition states to the extent of *ca.* 90% or more by the secondary process. Because the primary process involves the lesser amount of ligand motion in forming transition states, it is expected to represent a somewhat lower energy reaction pathway. Thus, the fit of the experimental kinetics with >90% s process may be fortuitous and, if so, suggests strongly that the SP-axial mechanism is not operative in the rearrangement reactions. This point is further emphasized by the recognition that the initial entity after bond rupture can equally well be visualized as B instead of A in the example given in Figure 8. In B the ring β, perpendicular to α, can rotate in two ways to form transition states **2***l* and **1**. Although B is unsymmetrical equal conversion to both transition states is highly probable and would lead to very nearly 50% s process.

(iii) **Mixed Transition States.** In the preceding two sections racemization and isomerization kinetics have been treated in terms of idealized, separate TBP and SP transition states. Because energy differences between these two geometries for a particular species are considered to be generally small,[37] the possibility exists that a transition state of one type might be formed and rearrange to another of different geometry before decaying to products. Formation of both TBP and SP transition states can be visualized in several ways. For example, an important characteristic of entity B in Figure 8 is that the plane of ligand β is approximately perpendicular to and bisecting that of ligand α. A TBP-axial transition state has this same property, and if it possessed an adequately long lifetime it could rearrange to an SP-axial transition state. Because the ligands α and β are effectively equivalent in this transition state, it is immaterial whether SP-axial reverts to TBP-axial or goes to products directly by a mixture of s and p processes, most probably in a 1:1 ratio. In order to treat this possibility, the microscopic rate constants are given in eq 19 as a function of the fraction t of TBP-axial transition states which pass to products without rearranging at any point to SP-axial transition states. The latter are assumed to decay to products in a 1:1 ratio of p and s processes. Predicted isomeriza-

$$k_1 = \frac{5}{16}(1 - t)k_c \qquad k_3 = \frac{5}{48}(1 - t)k_t \qquad k_5 = \frac{1}{16}(1 - t)k_c$$

$$k_2 = \frac{1}{16}(7 + t)k_c \qquad k_4 = \frac{1}{48}(7 + t)k_t \qquad k_6 = \frac{1}{48}(17 - t)k_t \tag{19}$$

$$k_{CT} = \frac{1}{4}(3 - t)k_c \qquad k_{TC} = \frac{1}{12}(3 - t)k_t$$

tion and racemization rates were calculated as in other cases and t was varied from 0 to 1. The results given in Table IX are consistent with the involvement of significant proportions of both transition states. The experimental k_2/k_1 or k_4/k_3 ratios are consistent with $t \cong 0.8$. Hence, some interconversion between the two types of transition states during the isomerization–racemization process cannot be excluded, but the majority of transition states responsible for the observed kinetics are of the TBP-axial type.

(37) E. L. Muetterties and R. A. Schunn, *Quart. Rev., Chem. Soc.*, 20, 245 (1966).

Conclusions. Racemization and isomerization of *cis*- and *trans*-Co(mhd)$_3$ in chlorobenzene solution obey first-order kinetics and are therefore intramolecular reactions.[38] This behavior is consistent with the results of Fay and Piper,[11] who found that Co(tfac)$_3$ and other M(tfac)$_3$ complexes undergo intramolecular isomerization in a number of organic solvents, and with those of Klabunde and Fay,[19] who have reported briefly that the rate of linkage isomerism in Co(triac-d_3)$_3$ and Co(triac-d_3)(acac)$_2$ is faster than the rate of ligand exchange in chlorobenzene. Isomerization and racemization of Co(mhd)$_3$ occur simultaneously and at comparable rates. The activation energies for these processes are practically identical (average value, 32 kcal/mol) and provide powerful support for a common reaction pathway, which is assumed in the foregoing predictions of rate ratios as a function of mechanism. It has been established that isomerization occurs stereoselectively, with inversion of configuration predominant. With reference to the processes given by eq 1, $k_2 > k_1$, $k_4 > k_3$, and $k_6 > k_5$.

Both bond-breaking and non-bond-breaking mechanisms have been investigated assuming geometrically idealized transition states. On the basis of the observations summarized in the preceding paragraph and comparison of actual and predicted rate constant ratios, the following pathways may be excluded as the sole reaction mechanism: (a) twist mechanism, (b) bond rupture producing TBP-equatorial transition states, (c) bond rupture producing TBP-axial transition states, (d) bond rupture producing SP-axial transition states which form products by the primary process. Twists about the real and pseudothreefold axes have been found not to be operative in rearrangement reactions of Cr(bzac)$_3$ and M(tfac)$_3$ complexes.[11] The following pathways are consistent with the rate constant data: (e) bond rupture producing about 90% TBP-axial transition states (kinetically indistinguishable from SP-basal); (f) bond rupture producing SP-axial transition states, which are formed to an extent of about 90% by the secondary process; (g) bond rupture producing mixtures of ~80% TBP- and ~20% SP-axial transition states, with the latter forming products equally by the primary and secondary processes. It can be readily shown that the experimental values of k_5 and k_6 are consistent with the above mechanisms. The available experimental information does not permit an unambiguous selection of any one of pathways e, f, and g as the most probable. However, for reasons stated earlier, any mechanism which requires production of SP-axial transition states predominantly by the secondary as opposed to the primary process is not considered likely; consequently, pathway f is regarded as quite improbable. It should be noted that the relative magnitudes of the microscopic rate constants and, therewith, predicted rate constant ratios and arguments based upon them are independent of any inherent differences in bond-rupture tendencies of the two ends of an unsymmetrical ligand such as mhd.[40]

The activation parameters summarized in Table IV for Co(mhd)$_3$ and related complexes do not afford unequivocal evidence for either of the pathways e and g, but appear to be consistent with a bond-rupture process. E_a and $\Delta H^{\ddagger}$ values are less than the energy (ΔH) to break homolytically a Co–O bond in Co(acac)$_3$[41] (51, 64 kcal/mol) as computed from heat of formation data. These quantities are the average energy per bond, and the energy necessary to break only one bond producing a five-coordinate species could conceivably be lower. Fay and Piper[11] have suggested that any twist mechanism should have a low preexponential factor because of the time necessary to channel the available energy into the proper vibrational modes. If this contention is valid, the relatively high preexponential factors for the first-order reactions of Co(mhd)$_3$ and Co(tfac)$_3$ would also argue against a twist mechanism. A relevant activation parameter is E_a = 39 kcal/mol for the linkage isomerization, **6** → **7** or the reverse, of Co(triac-d_3)$_3$ in chlorobenzene. If this

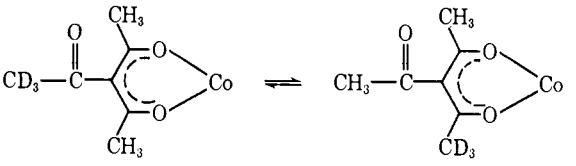

6 **7**

process is intramolecular the activation energy represents a reasonable estimate of that required for bond rupture in Co(mhd)$_3$. The difference of *ca.* 7 kcal/mol in the activation energies of the two complexes is not incompatible with the operation of a bond rupture mechanism in the rearrangments of Co(mhd)$_3$.

(38) This statement is correct provided that complete dissociation of one ligand does not occur. A dissociation mechanism of this sort has been suggested in the past to explain certain racemization processes,[10,39] but has been shown not to be operative in fast rearrangements of tris(β-diketonates).[13] As in other cases[11] this mechanism is rejected here because of the high activation energy required.

(39) W. Thomas, *J. Chem. Soc.*, 119, 1140 (1921).

(40) This statement is correct provided that the probabilities of metal–ligand bond rupture *within* each of the two sets (Co–OCMe, Co–OC-*i*-Pr) of three like bonds are equal. Assumption of exclusive rupture of one or the other of these two types of Co–O bonds leads to exactly the same kinetics. This is a consequence of the fact that *cis* and *trans* configurations are fixed by the relative positions of three bond labels (a–f), the positions of the remaining three necessarily being determined. The same isomer designation must be obtained whether the label is situated on the flagged or unflagged end of the ligand (*cf.* 2 and 3). There is a 1:1 correspondence between bonds to the flagged or unflagged ligand ends such that breaking either bond of a related pair produces identical products even though different transition states are involved. This situation may be appreciated by reference to **4** and **5**, which show trans-Λ (3) viewed from opposite ends of the p-C_3 axis. Vertices are designated according to the bond labeling schemes in Figures 7, 8, and 9. Note that moving all flags to the opposite ends of the ligands will interconvert **4** and **5**. The correspondence between b, e, f and d, a, c is demonstrated explicitly in the following interconversions for a TBP-axial mechanism (*cf.* Figure 7).

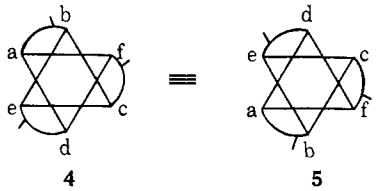

4 **5**

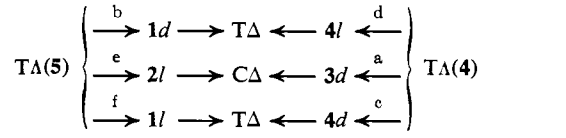

Transition states 1*d* and 4*l*, 2*l* and 3*d*, 1*l* and 4*d* can be interconverted by interchanging labeled and unlabeled ends of all ligands. A similar correlation exists between b, e, f and d, a, c for the other bond-breaking mechanisms discussed. Because exclusive rupture of either end of an unsymmetrical ligand leads to the same overall kinetics, any combination must also produce the same relative rates.

(41) M. M. Jones, B. J. Yow, and W. R. May, *Inorg. Chem.*, 1, 166 (1962); J. L. Wood and M. M. Jones, *ibid.*, 3, 1553 (1964).

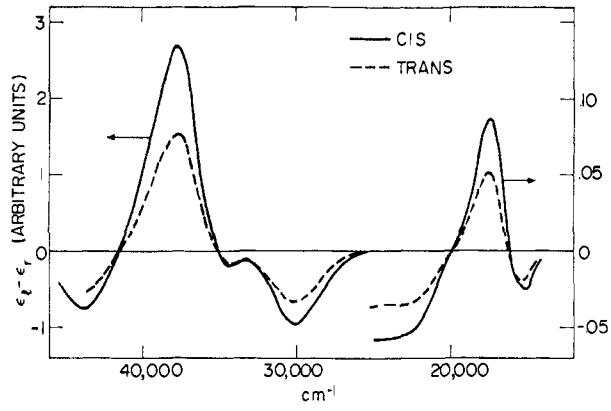

Figure 10. CD spectra of partially resolved *cis*- and *trans*-Co(mhd)$_3$ in cyclohexane solution: $[M]_{546}^{25}$ −7570° (*cis*), −2090° (*trans*). $\Delta\epsilon$ (37,700 cm^{-1}) 91.7 (*cis*), 23.7 l. mol^{-1} cm^{-1} (*trans*).

The kinetic analysis presented here is not intended to include all conceivable reaction mechanisms. Rather, the most physically plausible mechanisms, subject to reasonable restrictions, were examined in an attempt to determine whether or not the types of kinetic measurements described can sensibly distinguish one mechanism from another. More accurate isomerization data could possibly narrow further the set of acceptable mechanisms. The type of experiment which yielded the data in Table V, either carried out alone or coupled with more precise isomerization rates, can potentially lead to more accurate determination of all six microscopic rate constants. Such information would allow a somewhat more sensitive test of mechanisms than that permitted by the rate constant ratios employed here. The necessary experiments would be time consuming and would require larger quantities of equally or more highly resolved material than were obtained in this work.

Absolute Stereochemistry. The CD spectra of *cis*- and *trans*-(−)$_{546}$-Co(mhd)$_3$ are given in Figure 10. These spectra, like the absorption spectra, are very similar to each other and prove that the two levorotatory isomers have the same absolute configuration. In addition, they are essentially identical with that of fully resolved (−)$_{546}$-Co(acac)$_3$.[23b] In order to carry the definition of stereochemistry further, it would be desirable to relate the stereochemistry of the cobalt(III) complexes to that of (−)$_D$-[Si(acac)$_3$]$^+$. The absolute configuration of this ion is claimed to be Δ on the basis of an analysis of the optical activity of ligand π–π^* transitions.[42] The CD spectra of these species are similar in that they show a positive CD band in the 35,000–40,000-cm^{-1} region. At slightly lower energies [Si(acac)$_3$]$^+$ possesses a negative band nearly equal in area to the positive feature. In contrast, the cobalt(III) complexes show two negative CD bands in this region presumably deriving from the presence of several ligand transitions[23b] (*cf.* Table I), the identities and polarizations of which are unknown. Hence, it is not considered certain that the CD features found in the silicon cation correspond in terms of sign to those of cobalt(III) complexes with the same configuration. It can only be speculated that if the positive–negative sign behavior with decreasing energy in the π–π^* region is stereochemically diagnostic and the configuration of (−)$_D$-[Si(acac)$_3$]$^+$ is correct, (−)$_{546}$-Co(mhd)$_3$ and -Co(acac)$_3$ have the Δ configuration. It should be noted, however, that this conclusion does not agree with the assignment of the Λ configuration to tris-chelate complexes of (+)-hydroxymethylenecamphor[43,44] and related ligands.[45] The latter complexes contain the Co–O$_6$ chromophore and possess ligand-field absorption spectra similar in energy and intensity to those of Co(acac)$_3$ and Co(mhd)$_3$. Because of ligand stereoselective effects the most stable configurations of both *cis*- and *trans*-(−)$_{546}$-Co(+hmc)$_3$ are believed to be Λ. In the visible region (*ca.* 16,000–20,000 cm^{-1}) these complexes manifest similarly signed ORD and CD features when compared to (−)$_{546}$-Co(mhd)$_3$. An anomalous dispersion X-ray determination of the structure of an enantiomer of Co(acac)$_3$, which is the only neutral tris(β-diketonate) to have been fully resolved,[23b] would be extremely valuable in establishing absolute configurations of complexes of this type.

Acknowledgment. This research was supported by the National Science Foundation under Grant No. GP-7576X. We thank Drs. J. R. Hutchison and R. G. Bergman for valuable discussions, Dr. J. P. Collman for a copy of the thesis cited in ref 23, and Mrs. S. Eaton for experimental assistance. We are also indebted to Drs. J. W. Faller and M. Saunders for stimulating discussions concerning evaluation of rate constants from data of the sort presented in Table V.

(42) E. Larsen, S. F. Mason, and G. H. Searle, *Acta Chem. Scand.*, 20, 191 (1966).
(43) J. H. Dunlop, R. D. Gillard, and R. Ugo, *J. Chem. Soc. A*, 1540 (1966); A. J. McCaffery, S. F. Mason, and R. E. Ballard, *ibid.*, 2883 (1965).
(44) Y. T. Chen and G. W. Everett, Jr., *J. Amer. Chem. Soc.*, 90, 6660 (1968).
(45) G. W. Everett, Jr., and Y. T. Chen, *ibid.*, 92, 508 (1970).